JVI Journals.ASM.org

Mutations in the Capsid Protein of *Brome Mosaic Virus* Affecting Encapsidation Eliminate Vesicle Induction *In Planta*: Implications for Virus Cell-to-Cell Spread

Devinka Bamunusinghe,[a,b] Sonali Chaturvedi,[a] Jang-Kyun Seo,[a,c] A. L. N. Rao[a]

Department of Plant Pathology and Microbiology, University of California, Riverside, California, USA[a]; Laboratory of Molecular Microbiology, NIAID, National Institutes of Health, Bethesda, Maryland, USA[b]; Crop Protection Division, National Academy of Agricultural Science, Rural Development Administration, Suwon, South Korea[c]

Positive-strand RNA viruses are known to rearrange the endomembrane network to make it more conducive for replication, maturation, or egress. Our previous transmission electron microscopic (TEM) analysis showed that ectopic expression of wild-type (wt) capsid protein (CP) of *Brome mosaic virus* (BMV) has an intrinsic property of modifying the endoplasmic reticulum (ER) to induce vesicles similar to those present in wt BMV infection. In this study, we evaluated the functional significance of CP-mediated vesicle induction to the BMV infection cycle *in planta*. Consequently, the cytopathologic changes induced by wt CP or its mutants defective in virion assembly due to mutations engineered in either N- or C-proximal domains were comparatively analyzed by TEM in two susceptible (*Nicotiana benthamiana* and *Chenopodium quinoa*) and one nonhost (*N. clevelandii*) plant species. The results showed that in susceptible hosts, CP-mediated ER-derived vesicle induction is contingent on the expression of encapsidation-competent CP. In contrast, unlike in *N. benthamiana* and *C. quinoa*, transient expression of wt CP in nonhost *N. clevelandii* plants eliminated vesicle induction. Additionally, comparative source-to-sink analysis of virus spread in leaves of *N. benthamiana* and *N. clevelandii* coexpressing wt BMV and *Cucumber mosaic virus* (CMV) showed that despite *trans*-encapsidation, CMV failed to complement the defective cell-to-cell movement of BMV. The significance and relation of CP-mediated vesicle induction to virus cell-to-cell movement are discussed.

The onset of a given viral disease and its progression rely on coordinated strategies involving the host cell infrastructure and metabolism. Positive-strand RNA viruses pathogenic to humans, animals, and plants alter internal cellular membranes to create the physical scaffold offering the most suitable platform for virus replication (1–4). These alterations include intracellular modification of cellular organelles such as the endoplasmic reticulum (ER) by poliovirus (5), dengue virus (6), and *Brome mosaic virus* (BMV) and *Turnip mosaic virus* (TuMV) (7–9); mitochondria by *Flock house virus* (10, 11); lysosomes by *Semliki Forest virus* (12); and peroxisomes and chloroplasts by *Tomato bushy stunt virus* (13). Transmission electron microscopic (TEM) analysis of cells infected with positive-strand RNA viruses revealed that viral replication originates a variety of membrane structures, including from the formation of convoluted membranes and vesicle pockets; the proliferation of vesicular structures, including double-membrane vesicles; or the proliferation of spherule-like invaginations (5, 7, 14–16).

To facilitate understanding by readers, we wish to clarify the major differences between two terminologies: "vesicles" and "spherules." Vesicles (including double-membrane vesicles) and spherules differ morphologically. Vesicles are bubble-like structures derived from a cellular membrane, such as the ER; these are not physically connected to the cellular membrane and accumulate in the cytoplasm as large clusters surrounded by membranous sacs forming vesicle packets (3, 7). In contrast, like vesicles, spherules (3, 16) are also bubble-like structures derived from cellular organelles, such as the ER, mitochondria, or peroxisomes (3), but unlike vesicles, the outer membrane of spherules is physically connected to the cellular organelle through a narrow neck.

BMV, the type member of the *Bromoviridae* family, is a plant-infecting, multicomponent RNA virus with a single-stranded genome divided among three components: genomic RNA 1 (B1) and genomic RNA 2 (B2) are monocistronic sequences encoding replicase proteins 1a (p1a) and 2a (p2a), respectively; genomic RNA 3 (B3) is a dicistronic sequence and encodes a 5′ nonstructural movement protein (MP) and a 3′ structural capsid protein (CP) (17). CP is translated from replication-derived subgenomic RNA 4 (B4), which is synthesized from minus-strand B3 by an internal initiation mechanism (18). BMV ranks among the best-studied positive-strand RNA viruses with respect to replication and genome packaging (17, 19).

Establishment of a genetically amenable yeast (*Saccharomyces cerevisiae*) system has facilitated the evaluation and identification of the role of host factors and cellular membranes involved in the replication of BMV (16, 20–22). For example, results of genetic and biochemical studies showed that BMV replication occurs in perinuclear ER-derived spherules exclusively mediated by p1a; none of the other three viral genes (i.e., p2a, MP, and CP) are involved in ER modification (16). However, to date, these observations have not been validated *in planta*. In contrast, a recent study (7) involving the TEM analysis of *Nicotiana benthamiana* leaves infected with wild-type (wt) BMV or ectopically expressing either p1a, p2a, MP, or CP revealed three major scenarios contrasting to the scenario observed in the yeast system. First, wt BMV infection resulted in the accumulation of a collection of cytoplas-

Received 8 May 2013 **Accepted** 30 May 2013
Published ahead of print 5 June 2013
Address correspondence to A. L. N. Rao, arao@ucr.edu.

doi:10.1128/JVI.01253-13

mic ER-derived polymorphic vesicles arranged into patches. Second, no evidence for the induction of spherules in the perinuclear region, as was observed in yeast cells, was obtained. Third, unlike in yeast cells, ectopic expression of CP modified the ER to induce the accumulation of large assemblies of vesicles in the cytoplasm (7).

Given the intimacy between CP and viral movement (23–26), we hypothesized that remodeling of the ER by CP might play a critical role in packaging, movement, or pathogenesis (7). As a logical extension of these observations and to further evaluate the functional significance of CP-induced vesicles in the BMV infection cycle, the primary goal of this study was to identify the CP form (encapsidation competent versus incompetent) required for ER-derived vesicle induction in two susceptible (*N. benthamiana* and *Chenopodium quinoa*) and one nonhost (*N. clevelandii*) plant species. Since encapsidation-competent CP is an integral part of cell-to-cell movement (23–26), additional source-to-sink assays performed in *N. benthamiana* and *N. clevelandii* aided the evaluation of the intrinsic involvement of CP-induced vesicles in cell-to-cell movement.

MATERIALS AND METHODS

Transfer DNA (T-DNA) plasmid construction. Characteristic features of agrotransformants of three genomic RNAs of wt BMV RNA and wt subgenomic RNA 4 (B4) were described previously (27). Two CP mutants, Δ2-20 and F184A, constructed in this study, were derived from a binary plasmid (PZP) containing a BMV RNA 3 full-length cDNA clone using a PCR-mediated mutagenesis approach. To construct mutant CP Δ2-20, a PCR product was obtained using a forward primer (5′-ATGAATCGTTG GACCGCTAGGG-3′) and a reverse primer (5′-GGACTAGTTACCTAT AAACCGGGGTGAAG-3′; the SpeI site is underlined). To construct mutant CP F184A, a PCR product was obtained using a forward primer (5′-ATGTCGACTTCAGGAACTGG-3′) and a reverse primer (5′-GGAC TAGTTACTACCTATAAACCGGGGTGGCG-3′; the SpeI site is underlined). The resulting PCR products were digested with the restriction enzyme SpeI and subcloned into a 35S-B4.1 vector double digested with StuI and SpeI (27). The presence of the subcloned region in the desired orientation was confirmed by digestion with EcoRI and SacI followed by sequencing. The final recombinant plasmids are referred to as B4/Δ2-20 and B4/F184A, respectively (Fig. 1A and B).

Three CP mutants, 10P, 13P, and 18P, constructed in this study, were derived from cDNA clones of B3 harboring 10P, 13P, and 18P mutations, respectively (28). Each mutant sequence was amplified by a PCR using a forward primer (5′-GTATTAATAATGTCGACTTCAGGAA-3′) and a reverse primer (5′-GCACTAGTTGGTCTCTTTTAGAGATTTAC-3′; the SpeI site is underlined). The resulting products were digested with the restriction enzyme SpeI and subcloned to a 35S-B4.1 vector double digested with StuI and XbaI (27). The presence of the subcloned region in the desired orientation was confirmed by sequencing. The final recombinant plasmids are referred to as B4/10P, B4/13P, and B4/18P, respectively (Fig. 1A and B). The CP open reading frame (ORF) of each of these five mutants was amplified by PCR, and the resulting product was subcloned into an agroconstruct of full-length wt B3 as described above (27). The final recombinant plasmids are referred to as B3/Δ2-20, B3 F184A, B3/P10, B3/P13, and B3/P18 (Fig. 1A and B). All plasmid constructs were transformed into *Agrobacterium* sp. strain GV3101 cells before infiltration.

Agroinfiltration and electron microscopy. Leaves of *N. benthamiana*, *C. quinoa*, or *N. clevelandii* were infiltrated using either a single agrotransformant or a desired combination of agrotransformants as described previously (7, 10). For TEM analysis, infiltrated leaves were harvested at 4 days postinfiltration (dpi), fixed, and embedded in Spurr's resin as described previously (7, 10). Tissue sections approximately 50 nm thick were mounted onto nickel grids and then stained with 2% (wt/vol) aqueous uranyl acetate and lead citrate for 30 min before viewing under a transmission electron microscope (Tecnai 12 model instrument; FEI Co.) (7). The diameter of the vesicles was estimated as described previously (7).

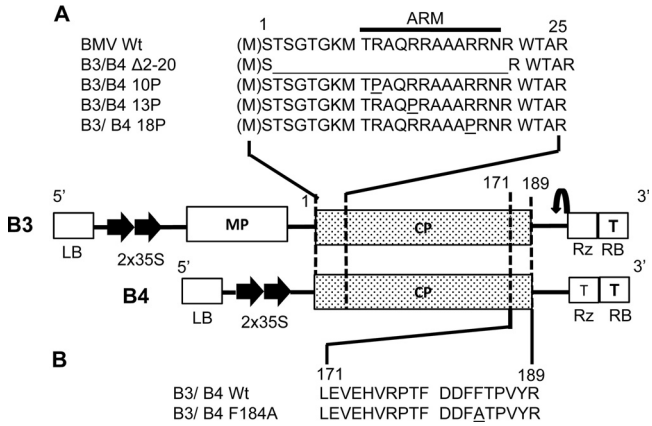

FIG 1 Characteristics of engineered mutations in the BMV CP ORF and schematic diagram of T-DNA-based BMV RNA 3 (B3) and the subgenomic RNA 4 (B4) agroconstructs. The basal binary vector, shown in the middle, contains, in sequential order, a left border of T-DNA (LB), a double 35S promoter (35S), full-length cDNA of either wt B3 or wt B4, a ribozyme sequence (Rz), a 35S terminator (T), and a right border of T-DNA (RB). Thin lines indicate noncoding regions. The open box and stippled boxes indicate the locations of the ORFs of BMV MP and CP, respectively. (A) Sequence encompassing the N-proximal 25-amino-acid region of the CP ORF in either B3 or B4 into which the indicated mutations were engineered. The location of the ARM is indicated. (B) Sequence encompassing the C-proximal amino acids located between positions 171 and 189 in the CP ORF of either B3 or B4. In mutant F184A, the amino acid phenylalanine (F) located at position 184 was replaced with alanine (A).

Progeny analysis. Protein extraction for immunoblot analysis and virion purification for TEM analysis were performed as described previously (7, 10). For analyzing virus or viral derivative progeny in source versus sink areas, agrocultures of either wt BMV or B4 were spot infiltrated into the leaves of *N. clevelandii* or *N. benthamiana*, as schematically shown in Fig. 7A and F. Leaf discs measuring about 4 mm were excised from the source and sink (approximately 30 mm from the source) at 4 and 7 dpi, respectively. Electron microscopic analysis of the purified virions following negative staining with uranyl acetate was performed as described above.

Coimmunoprecipitation assay (co-IP). *N. benthamiana* and *N. clevelandii* plants were infiltrated with agrocultures of BMV, *Cucumber mosaic virus* (CMV), or BMV plus CMV. At 4 dpi, virions were purified using methods that are specific for BMV (29) and CMV (30). Purified virions were then subjected to precipitation using anti-CP antibodies against BMV CP or CMV CP. Briefly, 20 μl of the desired anti-CP antibody was added to the purified virion preparation and the mixture was incubated at 4°C for 2 h with gentle shaking. Finally, anti-rabbit IgG (whole molecule)-agarose beads (Sigma) were used to specifically trap the immunoprecipitated virions. Western blot analysis was performed to confirm the specificity of the anti-CP antibodies. Coimmunoprecipitated virions were used to extract RNA, followed by reverse transcription-PCR (RT-PCR) using primers designed to amplify either a 500-nucleotide (nt) fragment of CMV RNA 1 or full-length BMV RNA 1, as described below.

***trans*-Encapsidation assay.** Following coinfiltration of wt components of BMV and CMV to either *N. benthamiana* or *N. clevelandii*, at 4 dpi, virions of BMV and CMV were purified according to the methods of Rao et al. (31) and Schmitz and Rao (30), respectively. Each virion preparation was subjected to co-IP using the respective anti-CP antibody in conjunction with anti-rabbit IgG-agarose (Sigma), and virion RNA was isolated by SDS-phenol-chloroform extraction. The isolated virion RNA

was identified by RT-PCR assays to determine if the packaging of heterologous RNA had taken place. Full-length BMV RNA 1 was amplified using a primer set consisting of a forward primer (5′-ATGTCAAGTTCT ATCGATTTGC-3′) and a reverse primer (5′-GGACTAGTCTTAACACA ATTA-3′) to yield a 3,234-nt product, while CMV RNA 1 was amplified using a forward primer (5′-CTAGTAAGCTTATGGCAACGTCCTCATT C-3′) and a reverse primer (5′-CCTAAGAATTCGCAAAAGTCCGGCT GGC-3′) to yield a 500-nt product.

RESULTS

Characteristic features of CP mutants used in this study. To verify whether CP-mediated vesicle induction in *N. benthamiana* plants is contingent on virus assembly, we selected a set of four mutants with mutations at their CP N termini (Fig. 1A) and one mutant with mutations at the CP C terminus (Fig. 1B) whose genetic makeups were as follows. Among these five mutants, two mutants, Δ2-20 and 184A, were assembly defective, while the remaining three mutants, 10P, 13P, and 18P, were assembly competent (28). Mutant Δ2-20 was characterized by lacking 19 N-proximal amino acids located between positions 2 and 20 (inclusive), which encompass an RNA binding arginine-rich motif (ARM; Fig. 1A). Mutant F184A (Fig. 1B) was assembly defective and characterized by the replacement of a C-proximal phenylalanine residue with an alanine residue (32). Mutants 10P, 13P, and 18P (Fig. 1A) were characterized by having a proline substitution for a positively charged arginine residue at the respective numeric positions located within the N-proximal ARM (28). As described in Materials and Methods, each of these mutant sequences was subcloned into the genetic background of T-DNA-based plasmids of either wt B3 (which translates CP from replication-derived mRNA when coexpressed with wt B1 and B2) or wt B4 (engineered to translate CP independently of replication; i.e., it has ectopic expression) (27) (Fig. 1A).

Ectopic expression of assembly-defective CP results in no vesicle induction. A previous TEM study involving ectopic expression of wt BMV CP in *N. benthamiana* plants revealed that the CP has a propensity to induce a large number of ER-derived vesicles arranged into vesicle packets (i.e., accumulation of clusters of vesicles into membrane sacs) (7). To identify the CP form (i.e., assembly competent versus incompetent) required for ER-derived vesicle induction, we performed the following experiment. *N. benthamiana* leaves were infiltrated with agrotransformants to ectopically express CP mutant B4/10P, B4/13P, B4/18P, B4/Δ2-20, or B4/F184A (Fig. 1A and B). Plants infiltrated with either wt B4, previously shown to ectopically express encapsidation-competent CP (27), or a full complement of wt BMV and those infiltrated with the empty vector (pCASS) alone served as appropriate positive and negative controls, respectively. Infiltrated leaves were harvested at 4 days postinfiltration (dpi) and divided into two lots: the first lot was used to verify the expression of CP by Western blotting and virion assembly, while the second lot was processed with Spurr's resin for visualizing membrane modifications by TEM (7). Although Western blot analysis confirmed the expression of CP in each case, virions characteristic of BMV could be purified from leaves expressing wt B4, B4/13P, B4/14P, or B4/18P but not from leaves expressing mutants B4/Δ2-20 and B4/F184A (data not shown), confirming that engineered mutations in Δ2-20 and F184A rendered the respective CP assembly deficient.

The results of TEM analysis of *N. benthamiana* leaves infiltrated with either wt BMV or wt B4 (positive controls) or ectopically expressing CP mutants (i.e., B4/13P, B4/14P, B4/18P, B4/Δ2-20, and B4/F184A) at 4 dpi are summarized in Fig. 2 and Table 1. TEM analyses of uninfiltrated leaves showed intact cellular organelles, such as the ER, chloroplast, mitochondrion, and nucleus (Fig. 2A). As reported previously (7), leaves expressing either a full complement of BMV or wt CP showed typical membrane modifications, including an ER-derived cluster of polymorphic, globular vesicles organized into vesicle pockets (Fig. 2B and C; Table 1). Induction of similar vesicle pockets was also observed in leaves ectopically expressing assembly-competent mutant B4/10P, B4/13P, or B4/18P (Fig. 2D to F). However, no such vesicle induction was observed in leaves expressing assembly-incompetent mutant B4/Δ2-20 or B4/F184A (Fig. 2G and H; Table 1). These modifications are not the artifacts of the chemical fixation used in this study, since the physical appearance and structure of cellular organelles, such as the Golgi apparatus, as exemplified in leaves infiltrated with wt BMV (Fig. 2A), remained unaltered. Taken together, these results suggest that CP-mediated vesicle induction requires an encapsidation-competent form of CP.

Expression of assembly-defective CP mutants via replication and their effect on vesicle induction. We have previously demonstrated that replication-derived CP exhibits a high degree of specificity in packaging viral RNA progeny (referred to as replication-coupled packaging), whereas ectopically expressed CP exhibits nonspecific packaging containing cellular RNA (27, 33). Therefore, to verify whether, similar to genome packaging, the ability to induce vesicles is also functionally coupled to replication, two assembly-defective mutants (i.e., Δ2-20 and F184A) or three assembly-competent mutants (i.e., 10P, 14P, and 18P) were subcloned into the genetic background of full-length B3, resulting in the construction of B3/Δ2-20, B3/F184A, B3/10P, B3/14P, and B3/18P (Fig. 1A and B). Each of these mutant B3 agrotransformants was mixed with wt B1 and B2 and used to coinfiltrate *N. benthamiana* leaves. At 4 dpi, each infiltrated leaf sample was divided into two lots. One lot was used to verify CP expression and virion assembly, while the second lot was used for TEM analysis for examining the cytopathologic changes induced by each CP mutant. Virion assembly similar to that for the wt control was observed for each of the CP mutants 10P, 13P, and 18P (Fig. 3A) but not for mutants Δ2-20 and F184A (Fig. 3B and C).

Results of TEM are summarized in Fig. 3D to F and Table 1. As shown in a representative example (Fig. 3D), vesicles induced by assembly-competent CP mutants 10P, 13P, and 18P were indistinguishable from those induced by the wt, and in each case, induction of vesicle pockets was clearly associated with dilated ER. Although ER-derived vesicle pockets were also induced in leaves expressing assembly-defective CP mutants Δ2-20 and F184A, a closer examination revealed that their morphology and appearance were clearly distinct from those induced by the wt and the assembly-competent CP mutants (Table 1). For example, as reported previously (7), the polymorphic vesicles induced by wt CP are oval (Fig. 3D), whereas those induced by either B3/Δ2-20 or B3/F184A are irregularly shaped (Fig. 3E and F; Table 1). For comparison, vesicle phenotypes induced by ectopically expressed p1a and CP are shown in Fig. 3G and H. Since the phenotypic appearance of vesicles induced in leaves coinfiltrated with B1, B2, and either B3/Δ2-20 or B3/F184A is identical to that of vesicles induced by p1a and p2a (7), we conclude that these vesicles were induced by p1a.

Vesicle induction by BMV CP mutants in *C. quinoa*. To verify whether the inability of assembly-deficient CP to induce vesicles is

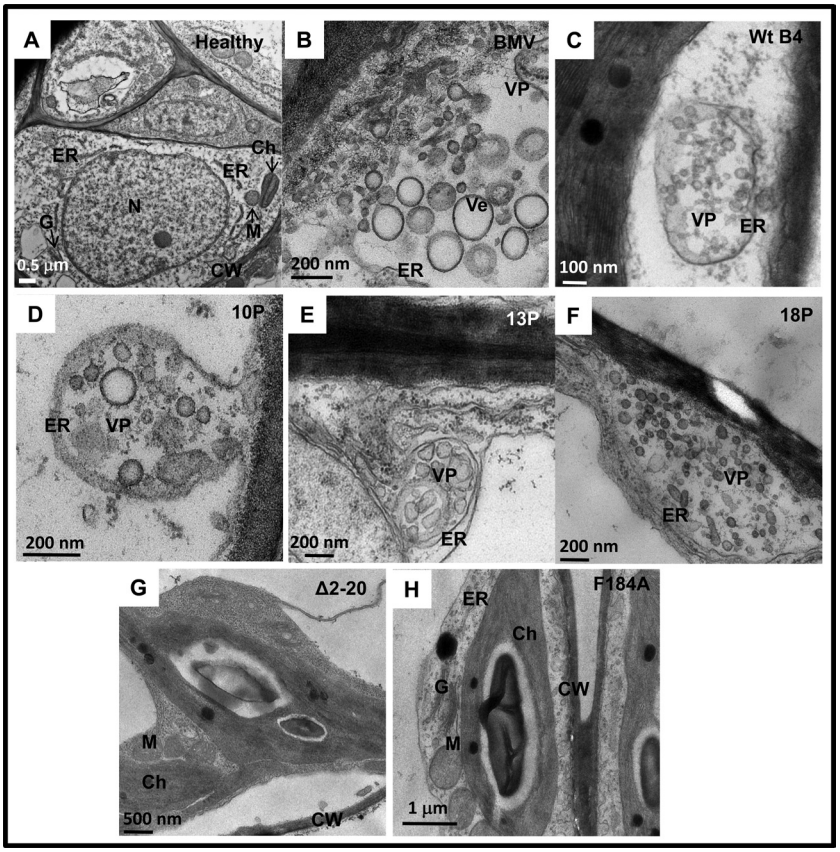

FIG 2 Membrane rearrangements in *N. benthamiana* cells induced by wt BMV, wt BCP, or BMV or BCP mutants. Representative TEM images of healthy leaves (A) or leaves agroinfiltrated with either wt BMV (B), wt B4 (C), B4/10P (D), B4/13P (E), B4/18P (F), B4/Δ2-20 (G), or B4/F184A (H) are shown. Following agroinfiltration at 4 dpi, the procedures used to fix the leaf tissue and for staining of thin sections are as described in Materials and Methods. N, nucleus; Ch, chloroplast; ER, endoplasmic reticulum; G, Golgi apparatus; M, mitochondrion; CW, cell wall; Ve, vesicles; VP, vesicle pocket.

a feature universally conserved *in planta*, we opted to test the effect of CP mutants in another host susceptible to BMV, *Chenopodium quinoa*. In contrast to healthy *C. quinoa* (Fig. 4A), wt BMV induced chlorotic local lesions followed by mottling symptoms on systemically infected uninoculated upper leaves (Fig. 4B) and supported efficient assembly of virions (Fig. 4C). Leaves of *C. quinoa* plants expressing either a full complement of wt BMV or wt CP from ectopically expressed B4 mRNA were subjected to TEM analysis. In contrast to healthy control leaves (Fig. 4D), infiltration of wt BMV (Fig. 4E) or ectopic expression of CP (Fig. 4F) resulted in vesicle induction similar to that observed in *N. benthamiana* plants (Fig. 2B and C). However, vesicle induction was never observed in leaves ectopically expressing assembly-defective mutants (data not shown). Taken together, these observations suggest that in susceptible hosts, ER-derived vesicle induction is contingent on the expression of assembly-competent CP.

TABLE 1 Characteristics of vesicles induced by wt and mutant BMV CP in *N. benthamiana*[a]

Inoculum	Vesicle induction	Diam (nm)[b]	Shape	Appearance	Origin	Vesicle pocket
B4[c]						
wt	+	56 ± 1	Oval	SM/Trs/Sta	ER	+
Δ2-20	−					
F184A	−					
B1-B2[d]						
B3	+	81 ± 2	Oval	SM/Trs/Sta/Cv	ER	+
B3/Δ2-20	+	77 ± 1	Irregular	SM/Trs/Sta		+
B3/F184A	+	87 ± 3	Irregular	SM/Trs/Sta	ER	+

[a] Vesicles or vesicle pockets induced by either B1-B2-B3/Δ2-20 or B1-B2-B3/F184A are due to replicase protein 1a (see the text for details). Abbreviations and symbols: SM, single membrane; Trs, Transparent; Sta, stained; Cv, convoluted (Bamunusighe et al., 2011); ER, endoplasmic reticulum; + and −, presence and absence of vesicles, respectively.
[b] Average diameters were calculated as described previously (Bamunusighe et al., 2011).
[c] wt and mutant CPs were expressed from ectopically expressed mRNA in the absence of replication.
[d] wt and mutant CPs were expressed from replication-derived mRNA.

wt CP is incompetent to induce ER modifications in nonhost *N. clevelandii* plants. As summarized in the introduction, in contrast to the cytopathology in *N. benthamiana* (7) or *C. quinoa* (this study; Fig. 4), one of the key features of BMV-induced cytopathology in a surrogate nonhost yeast system is the absence of CP-mediated vesicle induction (16). The reasons for this discrepancy are currently obscure. Since CP plays an important role in the cell-to-cell movement of BMV, the inability of BMV CP to induce vesicles could be one of the consequences of the defensive phenotypes associated with nonhosts. To verify this possibility and shed a light on the role of CP-mediated vesicle induction in cell-to-cell movement, we opted to use *N. clevelandii* as a nonhost experimental plant. The rationale for selecting *N. clevelandii* is as follows. The host range of BMV is largely restricted to the Gramineae family,

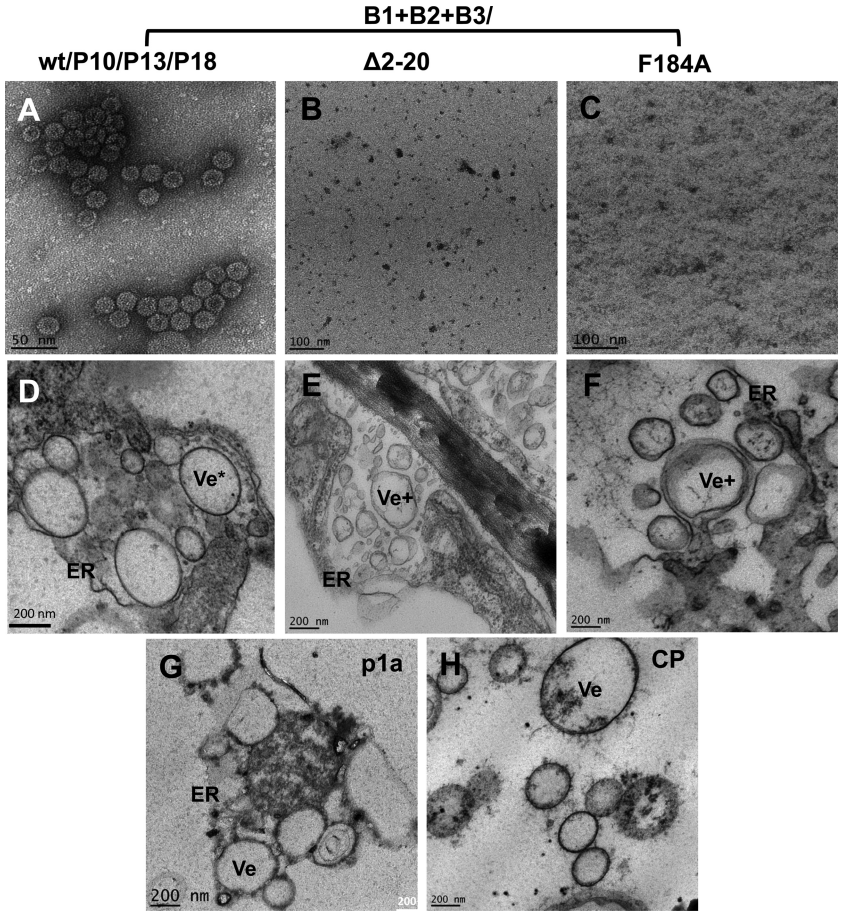

FIG 3 Assembly phenotypes and membrane rearrangements induced by wt BMV or its assembly-defective CP mutants in *N. benthamiana* leaves. (A to C) TEM images of negatively stained virions purified from leaves of *N. benthamiana* infiltrated with the samples indicated above the panels. (D to F) TEM images of vesicle induction in leaves infiltrated with the indicated samples. (G and H) TEM images of vesicles induced by transiently expressed p1a (G) or CP (H). ER, endoplasmic reticulum; Ve*, oval vesicles; Ve+ irregularly shaped vesicles.

but a limited number of species in other families have been reported to be susceptible (34). Among the members of the Solanaceae family, only *N. benthamiana* is susceptible to BMV infection, but it remains symptomless (35). In our preliminary attempts to infiltrate other members of the *Nicotiana* spp. that are resistant to BMV (34), such as *N. tabacum*, *N. glauca*, *N. glutinosa*, and *N. clevelandii*, only *N. clevelandii* was amenable for agroinfiltration (36), a process that allows synchronous delivery and expression of multiple plasmids into a single cell (27, 37). Although BMV does replicate in transfected cells of *N. clevelandii* (see Fig. 7A), it is classified as a resistant host since BMV infection remains subliminal. Therefore, we opted to use *N. clevelandii* as a nonhost plant species for examining the cytopathologic changes induced by BMV.

N. clevelandii leaves were infiltrated with a mixture of agrotransformants designed to ectopically express each BMV-encoded gene product, p1a, p2a, CP, or MP. Plants infiltrated with a mixture of all three wt BMV agrotransformants served as a control. At 4 dpi, leaves from infiltrated and uninfiltrated healthy plants were processed for TEM analysis, and representative images are shown in Fig. 5. The results are in contrast to those previously observed in *N. benthamiana* (7) or *C. quinoa* (this study; Fig. 4). First, in contrast to healthy leaves (Fig. 5A), *N. clevelandii* leaves infiltrated with wt BMV showed modified ERs associated with vesicle induc-

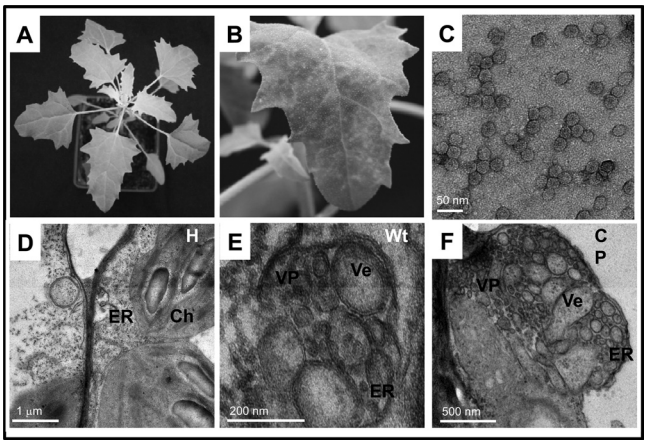

FIG 4 Symptom phenotypes and membrane rearrangements induced by wt BMV and its CP in *C. quinoa* leaves. (A) Healthy leaves; (B) a leaf systemically infected with BMV; (C) TEM image of negatively stained BMV virions purified from systemically infected *C. quinoa*. TEM images showing unmodified membranes in a healthy leaf (D) or membrane modifications induced by wt BMV (E) or ectopically expressed wt CP (F). Ch, chloroplast; ER, endoplasmic reticulum; VP, vesicle pocket; Ve, vesicle.

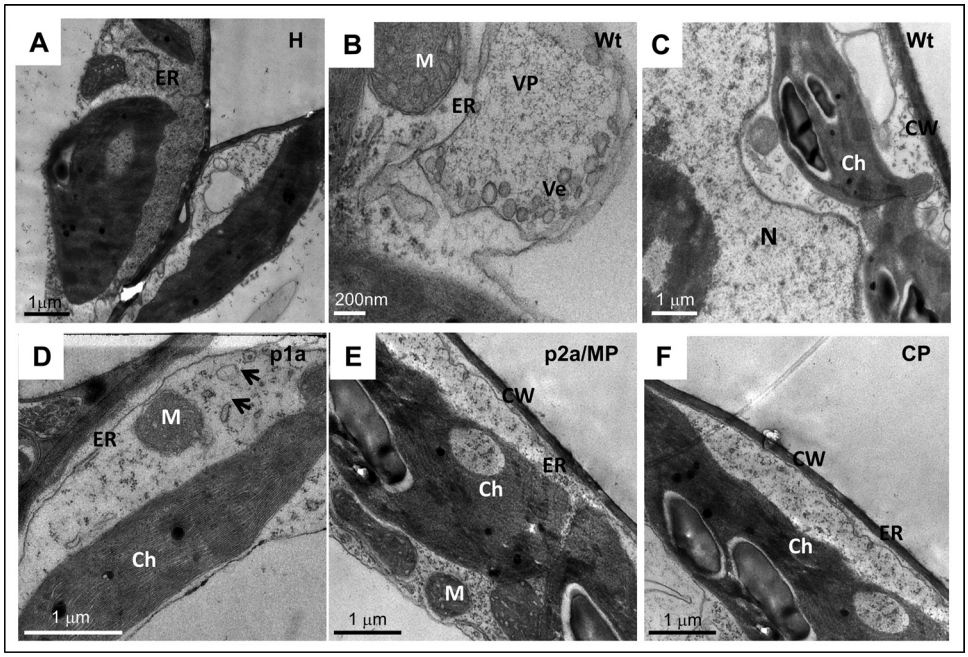

FIG 5 Representative TEM images showing the membrane rearrangements induced in healthy leaves of *N. clevelandii* (A) and leaves infiltrated with wt BMV (B, C), ectopically expressed p1a (D), p2a/MP (E), and CP (F). Ch, chloroplast; CW, cell wall, ER, endoplasmic reticulum; M, mitochondrion; N, nucleus; Ve, vesicle; VP, vesicle pocket.

tion and formed vesicle pockets (Fig. 5B). However, unlike in *N. benthamiana* (Fig. 2B) and *C. quinoa* plants (Fig. 4E), in *N. clevelandii* the number of vesicles induced by wt BMV in a given vesicle pocket was very low (Fig. 5B). Furthermore, no spherules were observed in any part of the cell, including the perinuclear region (Fig. 5C). Second, although vesicle induction by the expression of p1a was observed, the number of vesicles remained low (Fig. 5D). Third, the cytopathology of leaves expressing either p2a or MP was indistinguishable from that of healthy samples (compare Fig. 5A to E). Finally, the finding most significant to the present study was the absence of vesicle induction by the wt CP in *N. clevelandii* (Fig. 5F).

The results presented above clearly demonstrate that wt BMV CP is competent to induce vesicles in susceptible hosts such as *N. benthamiana* and *C. quinoa* but not in the nonhost *N. clevelandii*. The question that needs to be addressed is, what is the biological relevance of CP-mediated vesicle induction to the overall biology of the virus, specifically, to virus assembly and cell-to-cell spread? To find answers to this question, we compared the cytopathology, *trans*-encapsidation, and cell-to-cell spread of wt BMV when it was coexpressed with a genetically related virus, wt CMV, in *N. clevelandii*. Plants infected with wt BMV or wt CMV served as controls. The rationale for using CMV is as follows: first, both viruses possess a tripartite genome; second, unlike BMV, both *N. benthamiana* and *N. clevelandii* plants are susceptible to CMV; third, the cell-to-cell spread of both CMV and BMV requires CP in addition to MP (30, 38); and finally, the plant cellular membrane modifications involved in the replication of BMV and CMV are clearly distinct; i.e., BMV replication is associated with ER, while that of CMV is associated with tonoplasts (7, 39).

TEM images representing the cytopathologic changes induced in *N. clevelandii* plants following agroinfiltration with either wt CMV or wt BMV, or both, are shown in Fig. 6. Consistent with previous observations (39), *N. clevelandii* plants infected with CMV displayed induction of spherule-like invaginations associated with the tonoplast (Fig. 6A), while the ER remained unaltered. In contrast, as observed above (Fig. 5B), BMV infection resulted in the induction of few ER-derived vesicles (Fig. 6B).

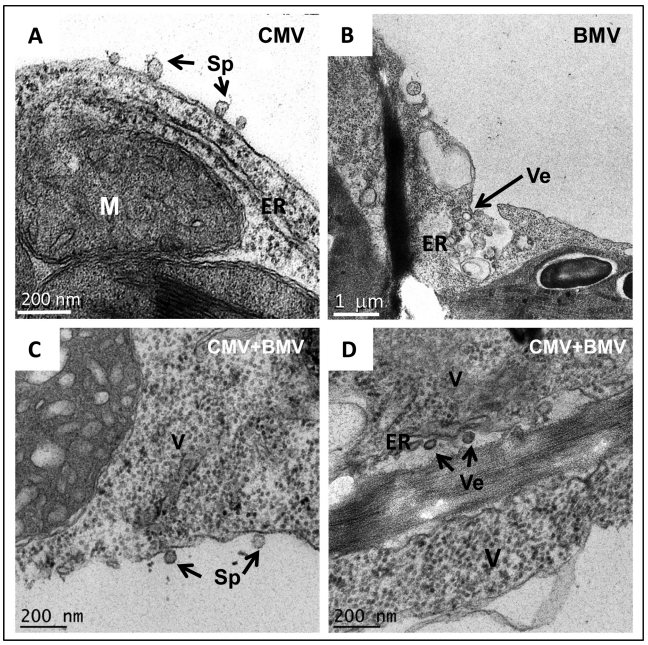

FIG 6 Representative TEM images showing membrane rearrangements induced in *N. clevelandii* by CMV (A), BMV (B), and CMV and BMV (C, D). M, mitochondrion; ER, endoplasmic reticulum, Sp, spherules; Ve, vesicles; V, virions.

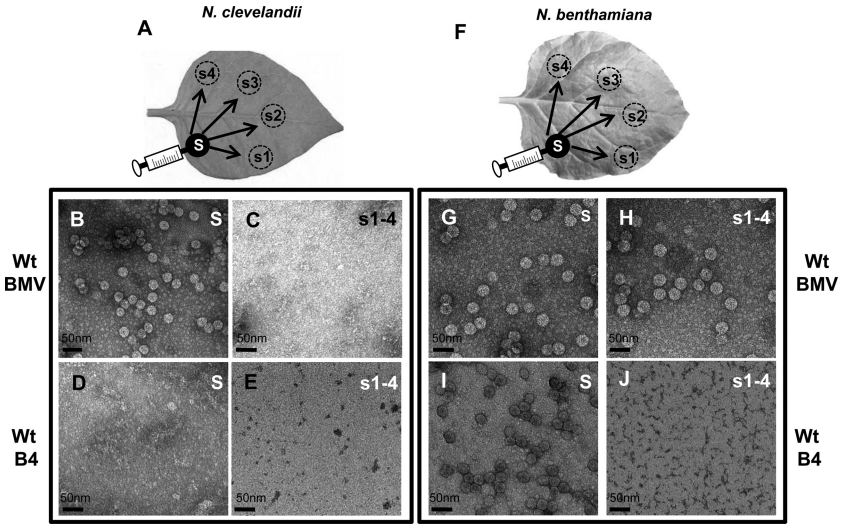

FIG 7 Assembly phenotype and cell-to-cell movement of wt BMV and ectopically expressed CP in *N. clevelandii* and *N. benthamiana*. Cultures of agrotransformants containing a full complement of either wt BMV or wt B4 were allowed to infiltrate either *N. clevelandii* (A) or *N. benthamiana* (F) as discrete spots referred to as the source (S; filled circles). Virions were purified from the source at 4 dpi and from four sink (s) spots (s1 to s4; dotted circles) at 10 dpi and examined by TEM. Representative TEM images of virion phenotypes assembled in the source and sink areas of *N. clevelandii* (B to E) and *N. benthamiana* (G to J) are shown.

Spherules associated with tonoplasts (characteristic of CMV; Fig. 6C) and few vesicles associated with ER (characteristic of BMV) were consistently detected in plants coinfected with CMV and BMV. In addition, the cytoplasm was inundated with electron-dense material resembling virus-like particles (Fig. 6C and D).

Interplay between CP-mediated vesicle induction and virus assembly. Since vesicle induction in *N. benthamiana* and *C. quinoa* plants requires assembly-competent BMV CP, the unexpected limited number of vesicles induced in *N. clevelandii* plants by wt BMV (Fig. 5B) or their absence induced by wt CP (Fig. 5F) prompted us to verify whether expression of wt BMV CP would result in the assembly of virions in *N. clevelandii*, as observed in *N. benthamiana* plants (27). To this end, an agrotransformant(s) containing a full complement of either wt BMV or B4 was allowed to infiltrate discrete spots (diameter, ~10 mm) in leaves of *N. clevelandii* (referred to as the source in Fig. 7A). An identical set of infiltrations performed in *N. benthamiana* plants (Fig. 7F) served as controls. At 4 dpi, a discrete set of leaf discs encompassing either the source or four sink areas (positioned approximately 30 mm away from the source) was excised from *N. clevelandii* and *N. benthamiana* leaves (Fig. 7A and F) and processed for virion purification followed by TEM examination. EM images are shown in Fig. 7B to J. Analysis of *N. clevelandii* leaves infiltrated with wt BMV revealed that only the spot representing the source (Fig. 7B) and none of the four spots representing sinks (Fig. 7C) contained virions characteristic of BMV. Since BMV is competent to move from cell to cell in *N. benthamiana* leaves (27), as expected, BMV virions were recovered from both source and sink regions in control leaves of *N. benthamiana* (Fig. 7G and H). These observations suggest that, unlike in *N. benthamiana* and *C. quinoa* (Fig. 2 and 4), vesicle induction by CP in *N. clevelandii* (Fig. 5F) is not related to virion assembly.

Interplay between CP-mediated vesicle induction and virus spread. Interesting results were obtained when BMV CP alone was ectopically expressed by allowing agrotransformant wt B4 to infiltrate *N. clevelandii* and control *N. benthamiana* leaves. BMV virions were not recovered from either the source (Fig. 7D) or sink (Fig. 7E) regions of *N. clevelandii* leaves. However, as observed previously (27), virions were recovered from the source (Fig. 7I) but not the sink (Fig. 7J) region of control *N. benthamiana* leaves. In BMV and CMV, in addition to MP, CP is obligated to promote cell-to-cell movement; however, BMV requires encapsidation-competent CP, while CMV does not (25, 30, 38). Despite efficient encapsidation, BMV was unable to move from cell to cell in *N. clevelandii* leaves (Fig. 7B and C). To verify whether CMV could complement the defective cell-to-cell movement of BMV, the following experiment was performed. Agrotransformants corresponding to wt genome complements of BMV and CMV were mixed and allowed to spot infiltrate (i.e., as the source) into *N. clevelandii* leaves. Similar infiltrations performed in *N. benthamiana* leaves served as controls (Fig. 8A and B). At 4 dpi, leaf discs were excised from the source and sink areas, as described above. Although the buffer compositions used to purify BMV and CMV virions were different (see Materials and Methods), initial Northern blot assays of virion RNA recovered from source areas revealed that the procedures used for the purification of BMV or CMV resulted in copurification of heterologous virions (data not shown). Therefore, a co-IP procedure using the respective anti-CP antibodies was used with the aim of precipitating virion RNA with the CP. In addition, this procedure allowed purification of BMV and CMV virions without cross-contamination (Fig. 8B). To further analyze the *trans*-encapsidation of heterologous RNAs, virion RNA isolated from co-IP preparations was subjected to RT-PCR using primers specific for genomic RNA preparations of either BMV or CMV (see Materials and Methods). A close analysis of the results summarized in Fig. 8C revealed the following: (i) BMV CP exhibited a high degree of packaging specificity, while CMV CP did not; (ii) as expected, in *N. benthamiana*, homologous virions of BMV and CMV packaging their respective genomic RNAs were detected in the source as well as in the sink areas, whereas in *N. clevelandii* CMV, virions packaging homologous RNA were detected in both the source and sink areas, while those of BMV were

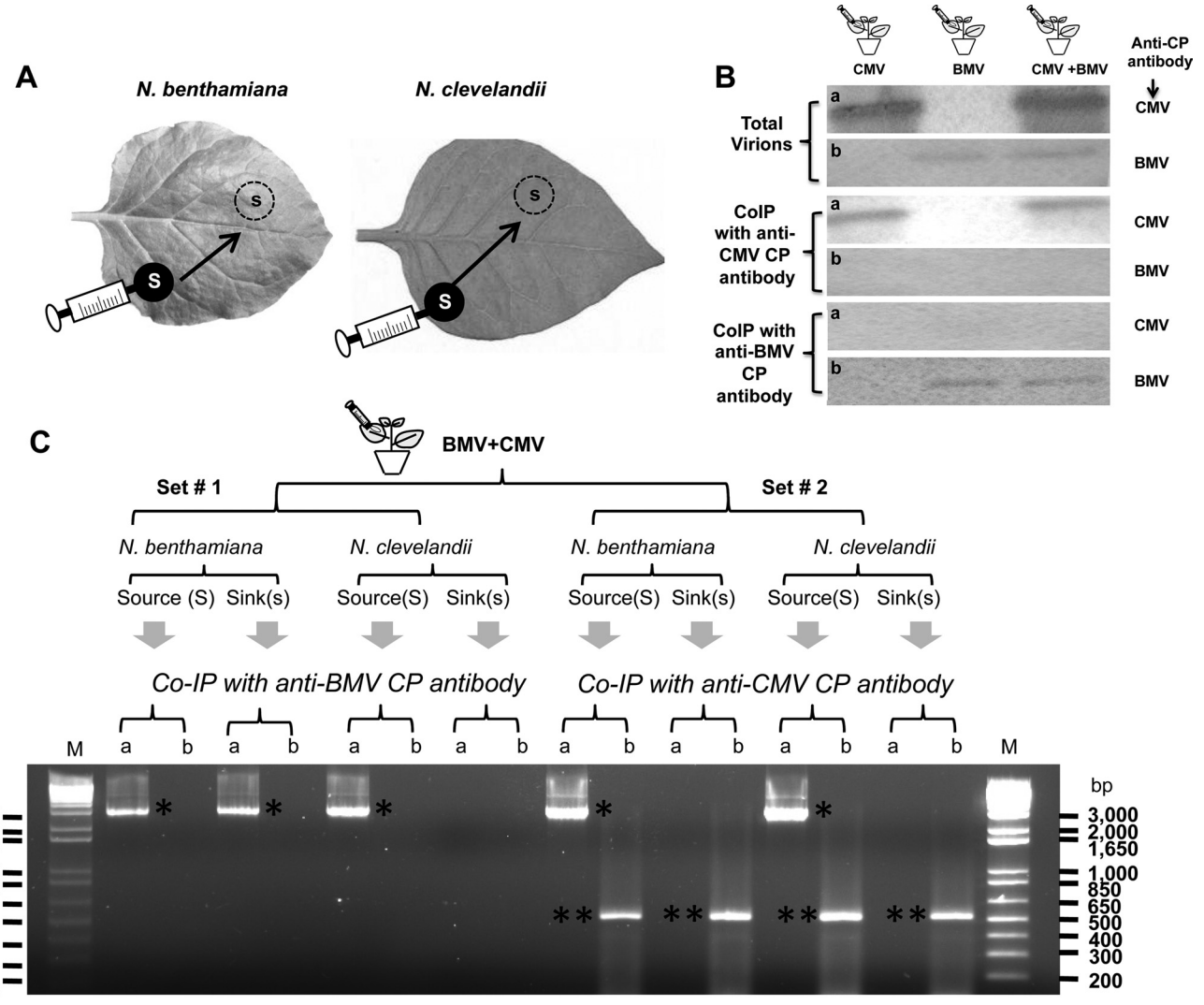

FIG 8 Coexpression of BMV and CMV in *N. benthamiana* and *N. clevelandii*. (A) Cultures of agrotranformants containing a full complement of wt BMV or wt CMV, or both, were allowed to spot infiltrate *N. benthamiana* or *N. clevelandii* as discrete spots referred to as the source (S; filled circles), and the progeny was analyzed from the sink (s; dotted circles). (B) Western blot analysis of BMV and CMV virions from coinfiltrated leaves by co-IP as described in Materials and Methods. Total virions purified from leaves infiltrated with BMV or CMV, or both viruses, were subjected to co-IP with either anti-CMV CP antibody or anti-BMV CP antibody. Precipitated virions were subjected to Western blot analysis by probing with either anti-CMV CP antibody (a) or anti-BMV CP antibody (b). (C) *trans*-Encapsidation assays. Leaves of *N. benthamiana* and *N. clevelandii* coexpressing BMV and CMV were divided into two sets (set 1 and set 2), as shown schematically. Virions purified from leaf discs about 15 mm in diameter excised from the source and sink areas were subjected to co-IP with either anti-BMV CP antibody or anti-CMV CP antibody. Virion RNA products isolated by co-IP were subjected to RT-PCR using primers designed to specifically amplify either the 3.2-kb full-length fragment of RNA 1 of BMV (a) or a 500-nt fragment encompassing the CMV RNA 1 sequence (b) (see Materials and Methods). The resulting PCR products were analyzed by agarose gel electrophoresis, followed by ethidium bromide staining. DNA size markers (lanes M) are shown to right and left of the gel. Single and double asterisks, electrophoretic mobility of PCR products corresponding to BMV RNA 1 and CMV RNA 1, respectively.

confined only to the source area; and (iii) despite the successful packaging of heterologous RNA, the failure to detect BMV RNAs in the sink areas suggested that CMV virions encapsidating BMV RNAs failed to move from the source to the sink. It is likely that encapsidation of BMV RNAs could have rendered the CMV virions functionally defective, preventing their interaction with the MP or cellular machineries (e.g., plasmodesmata) involved in virus cell-to-cell spread.

DISCUSSION

The major focus of this study was to identify the CP form required for vesicle induction *in planta*, followed by evaluation of the biological relevance of CP-mediated vesicle induction to the overall BMV infection cycle. The results show that only encapsidation-competent CP is able to induce vesicles in susceptible hosts *N. benthamiana* and *C. quinoa*, while in the nonhost *N. clevelandii*, even encapsidation-competent wt CP is not able to modify ER to induce vesicles. Additional source-to-sink assays revealed that BMV CP-induced vesicles are likely to play a significant role in prompting cell-to-cell transport of BMV. The implications and the biological relevance of these observations to the overall biology of BMV are discussed below.

In addition to playing a critical role in replication, rearrangement of cellular membranes by positive-strand RNA viruses is

critical for viral pathogenesis. In plant viruses, successful establishment of an infection requires efficient cell-to-cell movement that involves plasmodesmata in conjunction with the host cell endomembrane system (40, 41). Progress in dissecting virus movement at the cellular level made in the last decade revealed that many viruses traffic through the cellular endomembrane system (40–43). For example, the central domain of TGBp2 in the potexvirus *Potato virus X* (PVX), one of the three proteins required for virus movement, has been shown to induce vesicles budding from the ER network (44). Deletion of a conserved amino acid region from the central domain of TGBp2 eliminated the induction of ER-derived vesicles and inhibited virus cell-to-cell movement (45). Keeping these observations in perspective, we envision two likely roles for CP-induced vesicles. The first role is to promote virion assembly. In our previous study (7), we hypothesized that vesicles induced by CP might have a role in virion assembly. However, this study revealed that this is not the case. For example, unlike in *N. benthamiana* (27), although ectopically expressed CP in *N. clevelandii* is incompetent to modify ER to induce vesicles (Fig. 5F), expression of replication-derived CP readily resulted in assembly into virions (Fig. 7B). These observations suggest that virion assembly is linked to replication and occurs independently of vesicle induction. In positive-strand RNA viruses, genome packaging is functionally coupled to replication (10, 33, 46, 47), and this packaging specificity is regulated by a physical interaction between viral replicase and CP (48). Furthermore, we previously demonstrated that a mutant BMV CP assembled *in vivo* failed to assemble *in vitro* (49). Thus, it is likely that, in *N. clevelandii*, when BMV CP is expressed from a replication-derived mRNA, its interaction with replicase renders the CP assembly competent. Clearly, the absence of such an interaction between replicase and CP rendered the ectopically expressed CP assembly defective.

A second hypothesized role for CP-mediated vesicles is to promote cell-to-cell movement. Despite efficient replication in plant protoplasts, molecular and functional analyses of plant viral genes suggested that nonhost resistance to a given host is dictated by the incompatibility between the host machinery and the MP encoded by an RNA virus, thereby restricting the virus to initially infected cells (41). However, in a limited number of plant viruses, including BMV, cell-to-cell spread requires both MP and CP (25). Detection of tubules containing virus-like particles in protoplasts transfected with BMV suggested that BMV is likely to be transported between cells in fully assembled virion form by a tubule-guided mechanism (50), although there is no evidence yet that this mechanism prevails in plants. In addition to the virus-encoded MP and CP, a myriad of host proteins interacting with MP or CP aided by the host cell endomembrane system have been implicated in this active process (40, 41). The results of this study provide previously unrecognized cytopathology-based evidence to explain the mechanism of cell-to-cell movement of BMV. Apart from replication and assembly, the major differential phenotype exhibited by wt BMV in *N. benthamiana* and *N. clevelandii* is cell-to-cell movement. This defective cell-to-cell spread of BMV in *N. clevelandii* could be attributed to the defective MP resulting in subliminal infection. Alternatively, since cell-to-cell movement of BMV requires encapsidation-competent CP (25), compelling evidence for the conjecture that the cell-to-cell movement of BMV correlates with CP-mediated vesicle induction was obtained from the following observation: despite efficient virion assembly in *N. clevelandii* (Fig. 7B), BMV infection remained subliminal (Fig. 7C) and was correlated with the absence of CP-mediated vesicle induction (Fig. 5F). CMV is known to efficiently move from cell to cell in *N. clevelandii* (51). Furthermore, unlike BMV, the active process of cell-to-cell movement in CMV is mediated by the CP-RNA complex, and virion formation is not obligatory (30, 38). Therefore, we anticipated that CMV virions *trans*-encapsidating BMV RNAs (Fig. 8C) would move from cell to cell, but this was not the case (Fig. 8C). Although the reasons for this restricted cell-to-cell spread are not immediately obvious, a likely explanation would be that the structure of the CMV virions encapsidating BMV RNA is incompatible with the host machinery.

Since BMV CP predominantly localizes on the ER (7), it could interact with ER luminal factors such as small GTPases that regulate vesicle formation. These GTPases are crucial for budding of vesicles and for fusion with target membranes (52). If CP-mediated vesicles function as transport vesicles, it is reasonable to assume that they are functionally similar to plant transport vesicles. Another alternative explanation is based on our previous TEM evidence that pockets containing CP-induced vesicles are localized near plasmodesmata (7). As explained above, since virus assembly is not linked to vesicle induction, a possibility exists that these CP-induced vesicles might transport viral RNA to the cell surface. In this scenario, the vesicles could fuse with the cortical ER and release their contents into the plasmodesmata, promoting cell-to-cell transport. Experiments are in progress to substantiate this conjecture.

Finally, a comparative TEM analysis of cytopathologic changes induced in susceptible (*N. benthamiana* and *C. quinoa*) and nonhost (*N. clevelandii*) plant species supporting BMV replication revealed unexpected observations. It is worth noting that despite severe inhibition of ER-derived vesicle induction (compare Fig. 2B, 4E, and 5B, respectively, for *N. benthamiana*, *C. quinoa*, and *N. clevelandii*), the replication and assembly phenotypes of BMV in the nonhost species *N. clevelandii* are comparable to those in susceptible hosts (e.g., Fig. 7B and G). Previous two-dimensional ultrastructural analysis performed of plant cells infected with bromoviruses revealed the presence of ER-derived membranous vesicles (53–56). Since the vesicles seen in these studies did not resemble spherules, their existence in BMV (and other bromovirus)-infected plants remains open. Consequently, additional three-dimensional analysis is likely to clarify whether any of the vesicles seen in plant cells would represent spherules. Furthermore, a more realistic way of elucidating the existence of spherules associated with the BMV infection cycle would be to perform a side-by-side comparison of the membrane modifications induced by BMV in yeast and plant tissue. Another attractive way to unravel this dilemma would be to identify the specific host vesicle-associated protein (HVP) of the ER that promotes membrane invagination in *N. benthamiana* by genome-wide screening. Gain- and loss-of-function studies for the identified HVP genes in association with the analysis of BMV replication and cell-to-cell movement phenotypes are likely to provide valuable information to delineate the critical role of ER-derived membrane alterations not only in BMV replication but also in virus cell-to-cell movement (this study).

ACKNOWLEDGMENTS

We thank Deb Mathews for editorial comments.

This study was supported by a grant from the Committee on Research of the Riverside Division of the Academic Senate.

REFERENCES

1. **Denison MR.** 2008. Seeking membranes: positive-strand RNA virus replication complexes. PLoS Biol. **6:**e270. doi:10.1371/journal.pbio.0060270.
2. **Laliberte JF, Sanfacon H.** 2010. Cellular remodeling during plant virus infection. Annu. Rev. Phytopathol. **48:**69–91.
3. **Netherton CL, Wileman T.** 2011. Virus factories, double membrane vesicles and viroplasm generated in animal cells. Curr. Opin. Virol. **1:**381–387.
4. **Verchot J.** 2011. Wrapping membranes around plant virus infection. Curr. Opin. Virol. **1:**388–395.
5. **Schlegel A, Giddings TH, Jr, Ladinsky MS, Kirkegaard K.** 1996. Cellular origin and ultrastructure of membranes induced during poliovirus infection. J. Virol. **70:**6576–6588.
6. **Welsch S, Miller S, Romero-Brey I, Merz A, Bleck CK, Walther P, Fuller SD, Antony C, Krijnse-Locker J, Bartenschlager R.** 2009. Composition and three-dimensional architecture of the dengue virus replication and assembly sites. Cell Host Microbe **5:**365–375.
7. **Bamunusinghe D, Seo JK, Rao AL.** 2011. Subcellular localization and rearrangement of endoplasmic reticulum by Brome mosaic virus capsid protein. J. Virol. **85:**2953–2963.
8. **Grangeon R, Agbeci M, Chen J, Grondin G, Zheng H, Laliberte JF.** 2012. Impact on the endoplasmic reticulum and Golgi apparatus during Turnip mosaic virus infection. J. Virol. **86:**9255–9265.
9. **Restrepo-Hartwig M, Ahlquist P.** 1999. Brome mosaic virus RNA replication proteins 1a and 2a colocalize and 1a independently localizes on the yeast endoplasmic reticulum. J. Virol. **73:**10303–10309.
10. **Annamalai P, Rofail F, Demason DA, Rao AL.** 2008. Replication-coupled packaging mechanism in positive-strand RNA viruses: synchronized coexpression of functional multigenome RNA components of an animal and a plant virus in Nicotiana benthamiana cells by agroinfiltration. J. Virol. **82:**1484–1495.
11. **Miller DJ, Schwartz MD, Ahlquist P.** 2001. Flock house virus RNA replicates on outer mitochondrial membranes in Drosophila cells. J. Virol. **75:**11664–11676.
12. **Kujala P, Ikaheimonen A, Ehsani N, Vihinen H, Auvinen P, Kaariainen L.** 2001. Biogenesis of the Semliki Forest virus RNA replication complex. J. Virol. **75:**3873–3884.
13. **Barajas D, Jiang Y, Nagy PD.** 2009. A unique role for the host ESCRT proteins in replication of Tomato bushy stunt virus. PLoS Pathog. **5:**e1000705. doi:10.1371/journal.ppat.1000705.
14. **Knoops K, Kikkert M, Worm SH, Zevenhoven-Dobbe JC, van der Meer Y, Koster AJ, Mommaas AM, Snijder EJ.** 2008. SARS-coronavirus replication is supported by a reticulovesicular network of modified endoplasmic reticulum. PLoS Biol. **6:**e226. doi:10.1371/journal.pbio.0060226.
15. **Mackenzie J.** 2005. Wrapping things up about virus RNA replication. Traffic **6:**967–977.
16. **Schwartz M, Chen J, Janda M, Sullivan M, den Boon J, Ahlquist P.** 2002. A positive-strand RNA virus replication complex parallels form and function of retrovirus capsids. Mol. Cell **9:**505–514.
17. **Kao CC, Sivakumaran K.** 2000. Brome mosaic virus, good for an RNA virologist's basic needs. Mol. Plant Pathol. **1:**91–97.
18. **Miller WA, Dreher TW, Hall TC.** 1985. Synthesis of brome mosaic virus subgenomic RNA in vitro by internal initiation on (−)-sense genomic RNA. Nature **313:**68–70.
19. **Rao AL.** 2006. Genome packaging by spherical plant RNA viruses. Annu. Rev. Phytopathol. **44:**61–87.
20. **Chen J, Noueiry A, Ahlquist P.** 2003. An alternate pathway for recruiting template RNA to the brome mosaic virus RNA replication complex. J. Virol. **77:**2568–2577.
21. **Diaz A, Wang X, Ahlquist P.** 2010. Membrane-shaping host reticulon proteins play crucial roles in viral RNA replication compartment formation and function. Proc. Natl. Acad. Sci. U. S. A. **107:**16291–16296.
22. **Diez J, Ishikawa M, Kaido M, Ahlquist P.** 2000. Identification and characterization of a host protein required for efficient template selection in viral RNA replication. Proc. Natl. Acad. Sci. U. S. A. **97:**3913–3918.
23. **Rao AL.** 1997. Molecular studies on bromovirus capsid protein. III. Analysis of cell-to-cell movement competence of coat protein defective variants of cowpea chlorotic mottle virus. Virology **232:**385–395.
24. **Rao AL, Cooper B.** 2006. Capsid protein gene and the type of host plant differentially modulate cell-to-cell movement of cowpea chlorotic mottle virus. Virus Genes **32:**219–227.
25. **Rao AL, Grantham GL.** 1996. Molecular studies on bromovirus capsid protein. II. Functional analysis of the amino-terminal arginine-rich motif and its role in encapsidation, movement, and pathology. Virology **226:**294–305.
26. **Schmitz I, Rao AL.** 1996. Molecular studies on bromovirus capsid protein. I. Characterization of cell-to-cell movement-defective RNA3 variants of brome mosaic virus. Virology **226:**281–293.
27. **Annamalai P, Rao AL.** 2005. Replication-independent expression of genome components and capsid protein of brome mosaic virus in planta: a functional role for viral replicase in RNA packaging. Virology **338:**96–111.
28. **Choi YG, Rao AL.** 2000. Molecular studies on bromovirus capsid protein. VII. Selective packaging on BMV RNA4 by specific N-terminal arginine residuals. Virology **275:**207–217.
29. **Annamalai P, Rao AL.** 2008. RNA encapsidation assay. Methods Mol. Biol. **451:**251–264.
30. **Schmitz I, Rao AL.** 1998. Deletions in the conserved amino-terminal basic arm of cucumber mosaic virus coat protein disrupt virion assembly but do not abolish infectivity and cell-to-cell movement. Virology **248:**323–331.
31. **Rao ALN, Duggal R, Lahser FC, Hall TC.** 1994. Analysis of RNA replication in plant viruses, p 216–236. *In* Adolph KW (ed), Methods in molecular genetics: molecular virology techniques, vol 4. Academic Press, San Diego, CA.
32. **Okinaka Y, Mise K, Suzuki E, Okuno T, Furusawa I.** 2001. The C terminus of brome mosaic virus coat protein controls viral cell-to-cell and long-distance movement. J. Virol. **75:**5385–5390.
33. **Annamalai P, Rao AL.** 2006. Packaging of brome mosaic virus subgenomic RNA is functionally coupled to replication-dependent transcription and translation of coat protein. J. Virol. **80:**10096–10108.
34. **Lane LC.** 1981. Bromoviruses, p 333–376. *In* Kurstak E (ed), Hand book of plant virus infections and comparative diagnosis. Elsevier Biomedical Press, Amsterdam, Netherlands.
35. **Rao AL, Grantham GL.** 1995. A spontaneous mutation in the movement protein gene of brome mosaic virus modulates symptom phenotype in Nicotiana benthamiana. J. Virol. **69:**2689–2691.
36. **Choi SH, Seo JK, Kwon SJ, Rao AL.** 2012. Helper virus-independent transcription and multimerization of a satellite RNA associated with cucumber mosaic virus. J. Virol. **86:**4823–4832.
37. **Chaturvedi S, Jung B, Gupta S, Anvari B, Rao AL.** 2012. A simple and robust in vivo and in vitro approach for studying virus assembly. J. Vis. Exp. **61:**pii=3645. doi:10.3791/3645.
38. **Canto T, Prior DA, Hellwald KH, Oparka KJ, Palukaitis P.** 1997. Characterization of cucumber mosaic virus. IV. Movement protein and coat protein are both essential for cell-to-cell movement of cucumber mosaic virus. Virology **237:**237–248.
39. **Hatta T, Francki RI.** 1981. Cytopathic structures associated with tonoplasts of plant cells infected with cucumber mosaic and tomato aspermy viruses. J. Gen. Virol. **53:**343–345.
40. **Schoelz JE, Harries PA, Nelson RS.** 2011. Intracellular transport of plant viruses: finding the door out of the cell. Mol. Plant **4:**813–831.
41. **Scholthof HB.** 2005. Plant virus transport: motions of functional equivalence. Trends Plant Sci. **10:**376–382.
42. **Harries P, Ding B.** 2011. Cellular factors in plant virus movement: at the leading edge of macromolecular trafficking in plants. Virology **411:**237–243.
43. **Niehl A, Heinlein M.** 2011. Cellular pathways for viral transport through plasmodesmata. Protoplasma **248:**75–99.
44. **Ju HJ, Samuels TD, Wang YS, Blancaflor E, Payton M, Mitra R, Krishnamurthy K, Nelson RS, Verchot-Lubicz J.** 2005. The potato virus X TGBp2 movement protein associates with endoplasmic reticulum-derived vesicles during virus infection. Plant Physiol. **138:**1877–1895.
45. **Ju HJ, Brown JE, Ye CM, Verchot-Lubicz J.** 2007. Mutations in the central domain of potato virus X TGBp2 eliminate granular vesicles and virus cell-to-cell trafficking. J. Virol. **81:**1899–1911.
46. **Khromykh AA, Varnavski AN, Sedlak PL, Westaway EG.** 2001. Coupling between replication and packaging of flavivirus RNA: evidence derived from the use of DNA-based full-length cDNA clones of Kunjin virus. J. Virol. **75:**4633–4640.
47. **Nugent CI, Johnson KL, Sarnow P, Kirkegaard K.** 1999. Functional coupling between replication and packaging of poliovirus replicon RNA. J. Virol. **73:**427–435.
48. **Seo JK, Kwon SJ, Rao AL.** 2012. A physical interaction between viral replicase and capsid protein is required for genome-packaging specificity in an RNA virus. J. Virol. **86:**6210–6221.

49. **Calhoun SL, Speir JA, Rao AL.** 2007. In vivo particle polymorphism results from deletion of a N-terminal peptide molecular switch in brome mosaic virus capsid protein. Virology **364:**407–421.
50. **Kasteel DT, van der Wel NN, Jansen KA, Goldbach RW, van Lent JW.** 1997. Tubule-forming capacity of the movement proteins of alfalfa mosaic virus and brome mosaic virus. J. Gen. Virol. **78**(Pt 8):2089–2093.
51. **Palukaitis P, Garcia-Arenal F.** 2003. Cucumoviruses. Adv. Virus Res. **62:**241–323.
52. **Jurgens G.** 2004. Membrane trafficking in plants. Annu. Rev. Cell Dev. Biol. **20:**481–504.
53. **Burgess J, Motoyoshi F, Fleming EN.** 1974. Structural changes accompanying infection of tobacco protoplasts with two spherical viruses. Planta **117:**133–144.
54. **Francki RIB, Milne RG, Hatta T.** 1985. Bromovirus group, vol II. CRC Press, Inc, Boca Raton, FL.
55. **Kim KS.** 1977. An ultrastructural study of inclusions and disease development in plant cells infected by cowpea chlorotic mottle virus. J. Gen. Virol. **35:**535–543.
56. **Paliwal YC.** 1970. Electron microscopy of Bromegrass mosaic virus in infected leaves. J. Ultrastruct. Res. **30:**491–502.